EFFECT OF BURIED EXPLOSIONS

Bibiana M. Luccioni[a,c] and Ricardo D. Ambrosini[b,c]

[a]Instituto de Estructuras, Universidad Nacional de Tucumán, Av. Roca 1800, 4000 S.M. de Tucumán , Argentina, labest@herrera.unt.edu.ar.edu.ar , www.herrera.unt.edu.ar/iest
[b] Facultad de Ingeniería, Universidad Nacional de Cuyo
Centro Universitario - Parque Gral. San Martín - 5500 Mendoza, dambrosini@uncu.edu.ar , http://fing.uncu.edu.ar/
[c]CONICET, Av Rivadavia 1917, Cdad de Bs As

Keywords: Crater, blast load, soil, hydrocode, damage

Abstract. Shallow buried explosives pose a significant threat to lightweight vehicles and their occupants. Short term loading imparted by the explosion is enormously complex and can be significantly affected by a number of parameters including the size, shape, type, detonation point and depth of burial of the explosive and the type of soil. Extensive research activities in the field of buried blast loads have taken place in the last few decades. Nevertheless, the knowledge about the effect on objects placed over the ground is still limited. Most results are restricted to experimental observations or what have occurred during actual blast events.

Recent advances in numerical simulation have enabled the blast of buried explosives to be simulated. The accuracy of numerical simulation of craters produced by underground explosions was proved in a previous paper. The numerical analysis of crater formation due to underground explosions was performed with a hydrocode. Further validation of the modeling technique is considered in the current paper. First, the crater produced by spherical explosives loads varying from 10 to 100 kg of TNT, placed at different depths, are simulated and compared with experimental results. Then the effect on objects located at the ground level and over the ground is analyzed. The paper is completed with comparison with experimental results and numerical results obtained by other researchers.

1 INTRODUCTION

Blasting loads have come into attention in recent years due to the great number of accidental or intentional events that affected important structures all over the world, clearly indicating that the issue is relevant for purposes of structural design and reliability analysis. In consequence, extensive research activities in the field of blast loads have taken place in the last decades (Alia and Souli 2006, Ambrosini et al 2002). Between all blast events, undrground explosions have been given special attention.

Underground reinforced concrete structures are used for essential installations protected against the effects of conventional weapons (Wang et al 2005). Usually such structures are box shaped, partially or fully buried. The physical processes that govern the response of the underground structure are very complex, involving dynamic interactions among the explosive, the soil and the underground structure. Major phenomena include the formation of the crater or camouflet by the explosion; the propagation of the shock wave and elastic–plastic wave in the soil; and the interaction between soil and the structure.

By the other side, according to the 1999 Landmine Monitor report from the International Committee to Ban Landmines, estimates on the number of buried landmines worldwide range from 60 to 110 million (Cheeseman 2006). Both armoured personnel carriers and light combat vehicles are increasingly being used in a support role for other, more heavily armoured combat vehicles, all of which are being subjected to much greater risk from a variety of highly lethal antitank land mines (Gupta 1999) . Protective equipment, either for personnel or vehicles, must be designed to mitigate the effect of a landmine blast (Cheeseman 2006). As a result, there is a need for modelling and understanding the interaction of mine blast products with structures and the resulting loading and damage mechanisms inflicted by explosive blast and impact. This understanding is required both for damage assessment and protective hardening of both wheeled and tracked vehicles.

A cavity is always formed when a confined explosion is produced in a mass of soil (sw). The mechanics of explosive crater formation are complex and are related to the dynamic physical properties of the air, the subgrade and the air/ground interface. Even carefully controlled cratering experiments have deviations in measured crater dimensions of 210%, while scatter in the range of230±40% is common (Bull and Woodford 1999)

Apparent crater size prediction curves are available for wet clay, moist clay, dry clay, wet sand, dry-to-moist sand, loess, silt, frozen ground, basalt, shale, ice and snow (Bull and Woodford 1999). The term apparent crater refers to the crater as it appears immediately following the explosion. It is easy to measure the apparent crater.

If the explosion is close to the surface, a crater is formed, a complex interaction taking place between gravity effects, soil strength and transient load conditions. The most important variables in defining the crater shape and size are the mass W of the explosive and the depth of the detonation beneath the air/soil interface d. When $d < 0$, the explosive is detonated over the air/soil interface, $d = 0$ when the detonation occurs in the air/soil interface and $d > 0$ when the explosive is detonated beneath the soil surface. For $d > 0$, the crater mechanism is altered by gravitational effects. When the depth of the detonation increases, larger amounts of subsoil must be expelled by the explosion. Thus the crater radius and the depth of the crater increase when d increases, until a certain limit value, from which they rapidly decrease (Bull and Woodford 1999). Studies concerned with the characteristics of craters caused by explosions usually resort to dimensional analysis and statistics. The scaling law establishes that any linear dimension “L” of the crater can be expressed as a constant multiplied by W^{α} divided by the distance of the charge from the ground, where W represents the equivalent TNTmass of

explosive and α is a coefficient depending upon if gravitational effects can be neglected or not. In the first case the cubic root lawis applicable (α = 0.33) and in the other cases the functional dependence can be quite complex.

The authors have conducted a series of tests performed with different amounts of explosive at short distances above and below ground level, as well as on the soil surface are briefly described.(Ambrosini et al 2002).

They also presented (Ambrosini and Luccioni 2006a) a numerical study on craters formed by explosive loads located on the soil surface is presented. The soil parameters used in the numerical model, as well as the analysis procedure, were validated against experimental observations of the crater diameters. Moreover, the effect of elevation of the centre of energy release of explosive loads located on the soil surface were analyzed and discussed. Simple predictive equations for the crater diameter were presented.

In a recent paper the accuracy of numerical simulation of craters produced by underground explosions was proved (Luccioni and Ambrosini 2006). For this purpose, the numerical analysis of crater formation due to underground explosions was performed with a hydrocode. Several numerical approaches were carried out using different models and processors for the soil. Moreover, different alternatives for the constitutive model of the soil were used.In order to validate the numerical approach and prove its ability to model the crater formation, comparison with experimental results is performed. Many simulations of the same physical model lead to the same crater dimensions and a good agreement between the test results and the predicted crater measures was achieved.

Both papers (Luccioni and Ambrosini 2006 and Ambrosini and Luccioni 2006) demonstrated that the elastic properties of the soil do not significantly affect the diameter of the crater obtained. It was also proved that when the failure limit and the yield function are changed between reasonable limits, the diameter of the crater remains unchanged.

Nevertheless, it is well know that transmission of blast waves through soil layers and consequently their effect on underground structures or structures placed on or over the ground is strongly dependent on soil properties.

When a high explosive is detonated an inward wave is generated in the explosive material, at the same time, a shock wave moves through the surronding medium, which is at lower pressure and a contact discontinuity appears between the rarefaction wave and the shock wave. Experiments have shown (Alia and Souli 2006) that the resulting flow is quite complex, involving several physical phenomena as burning effects and heat transfer. The detonation of high explosive material converts the explosive charge into gas at high pressure and temperature what leads to damage structures. The physical processes during an explosion in soil and the subsequent response of buried and overground structures are extremely complex. Combining all these processes into a single analysis model involves several numerical difficulties but such a model will enable more realistic reproduction of the underlying physical processes. The nonlinear properties and large deformation of the soil and reinforced concrete make the whole physical process highly nonlinear, both in terms of the material and geometric nonlinearities (Wang et al 2005). Numerical simulations help to minimise the number of tests required that are very costly, and also help to interpret test results. Once simulations are validated by test results, it can be used as design tool for the improvement of the system structure involved.

Further validation of the modeling technique previously prsented is considered in the current paper. First, the crater produced by spherical explosives loads varying from 10 kg of TNT to 100kg of TNT, placed at different depths, are simulated and compared with experimental, empirical and numerical results obtained by other researchers. Then the blast

wave propagation through soil and effect on objects located over the ground is analyzed. Numerical results are compared with empirical and numerical results found in the literature.

2 CRATER FORMATION

2.1 Introduction

The prime factors in determining crater size and shape are the mass W of the explosive, the position λ_c of the explosive at detonation and the medium within which it is detonated (Bull and Woodford 1999). λ_c is the depth of detonation beneath the air/ground interface divided by $W^{0.33}$. Often different scaling law powers are used, for example where the radius is related to $W^{0.33}$and the depth related to $W^{0.33}$. The resulting crater will have one of three shapes detonated (Bull and Woodford 1999). A conventional crater shape is when $0.2<\lambda_c<0.8$, (see Fig 1)., a partial camouflet when $0.8<\lambda_c<1.4$ and a camouflet like that shown in Figure 2 when $\lambda_c \geq 1.4$. The camouflet comprises a spherical void with a highly compacted subgrade shell around it. Above the camouflet a conical shaped volume of subgrade had been displaced upwards, loosened and resettled. Figure 2 (Bull and Woodford 1999) shows a section through the camouflet with the zones, numbered 1 to 8 indicating different damage of the subgrade.

For $\lambda_c > 0$ gravity effects alter the mechanism of crater formation. Increasing the depth of detonation means that the explosive energy has to overcome increasing amounts of overburden and the corresponding tensile properties of the subgrade. Consequently, the apparent crater radius and apparent crater depth increase with decreasing λ_c until an unspecified value of lc has been reached. Then the apparent crater radius and apparent crater depth begin to decrease as increasing amounts of material, initially expelled from the crater, fall back. The maximum apparent crater is formed when $0.4<\lambda_c<0.6$.

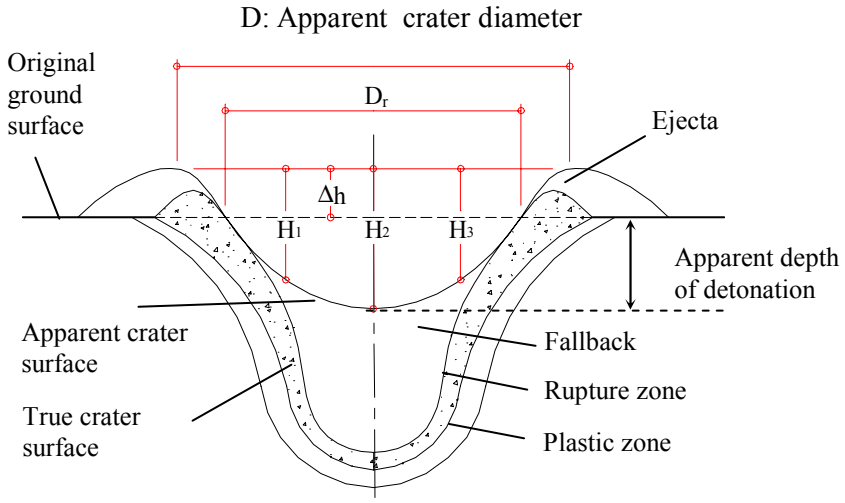

Figure 1: Conventional Crater

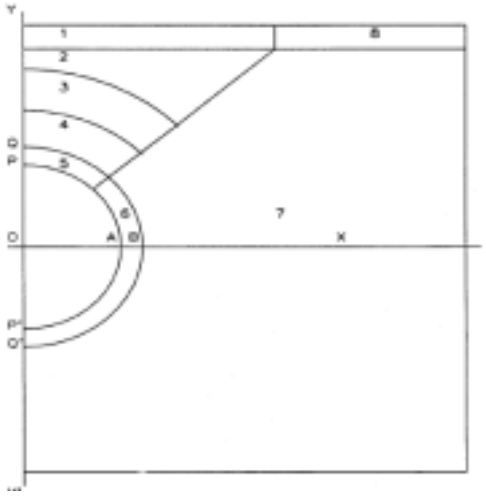

Figure 2: Camouflet (Bull and Woodford 1999)

2.2 Problem analyzed

First a test is modeled and results are compared with experimental results. Once the ability of the numerical model has been checked, the depth of the explosive is varied, maintaining all the other properties, and the resulting craters dimensions are compared with experimental and empirical values. The different shapes of craters and camouflets are analyzed.

In order to carry out a comparable analysis, the mass of the explosive is defined by TNT masses. The corresponding masses for other explosives can be obtained through the concept of TNT equivalence (Formby, 1996).

A spherical explosive load of 10 kg of TNT buried 98 cm below the soil level is first modeled. Then the depth is varied. The detonator is supposed to be in the centre of the TNT spherical charge.

The test were performed in a soil with following profile (Ambrosini et al 2002),

1)0 to 0.70 m Brown clayey silt with organic matter.

2)0.70 to 5.0 m Reddish brown clayey silt of low plasticity, classification CL, very dry. All the results are obtained for this soil.

Figure 3 shows a photograph of the crater experimentally obtained for this case (Ambrosini et al 2002). The apparent crater diameter was $D = 3.93\text{m}$.

2.3 Numerical modeld

The analysis is performed with a hydrocode (AUTODYN v6.1).

The symmetry conditions allow using a two-dimensional (2D) mesh considering axial symmetry. A 5m x 2.5m mesh with a minimum 10mm x10mm size was used. This mesh represents an m-diameter cylinder. The mesh was filled with different materials: air, TNT and soil, indicated with different colors in Figure 4. The mesh was refined with 1 cm cell all around the estimated final crater. Then, the maximum error in the final diameter of the crater is 2 cm and the maximum error in the depth is 1 cm.

Figure 3. Experimental crater

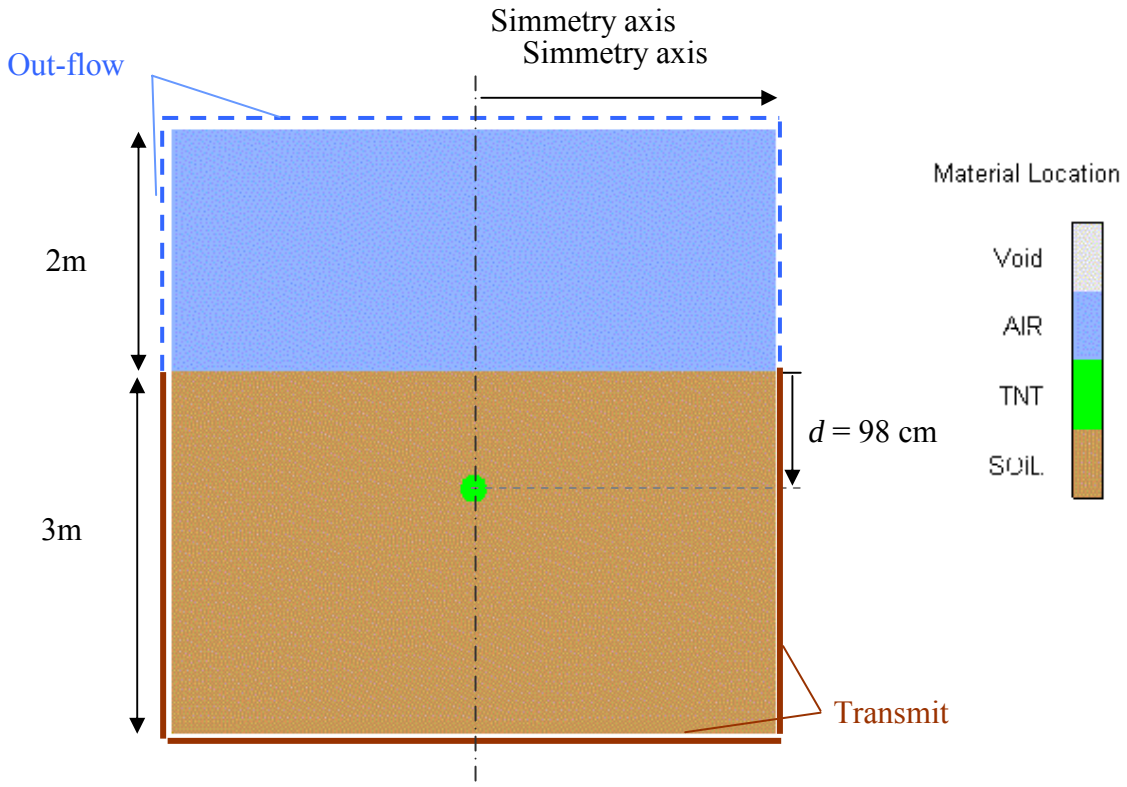

Figure 4: Numerical model. (10 kg of TNT at 98 cm depth)

An n Euler Godunov multi material (Alia and Souli 2006) with strength higher order processor is used to model the complete problem including the air, the explosive charge and the soil.

The ideal gas equation of state was used for the air. This is one of the simplest forms of equation of state for gases. In an ideal gas, the internal energy is a function of the temperature alone and if the gas is polytropic the internal energy is simply proportional to temperature. It follows that the equation of state for a gas, which has uniform initial conditions, may be written as,

$$p = (\gamma - 1)\rho e \tag{1}$$

in which p is the hydrostatic pressure, ρ is the density and e is the specific internal energy. γ is the adiabatic exponent, it is a constant (equal to $1 + R/c_v$) where constant R may be taken to be the universal gas constant R0 divided by the effective molecular weight of the particular gas and c_v is the specific heat at constant volume. The values of the constants used for air are presented in Table 1.

Equation of State: Ideal gas
$\gamma = 1.4$
Reference density: $\rho_a = 1.225\ 10^{-3}$ g/cm^3
Reference temperature: $T_o = 288.2$ K
Specific heat: $c_v = 717.3$ J/kgK

Table 1: Air properties

Lee-Tarver equation of state (Lee and Tarver, 1980) was used to model both the detonation and expansion of TNT in conjunction with "Jones - Wilkins - Lee" (JWL EOS) to model the unreacted explosive.

The (JWL) equation of state can be written as,

$$p = C_1\left(1-\frac{\omega}{r_1 v}\right)e^{-r_1 v} + C_2\left(1-\frac{\omega}{r_2 v}\right)e^{-r_2 v} + \frac{\omega e}{v} \qquad (2)$$

Where $v = 1/\rho$ is the specific volume, C_1, r_1, C_2, r_2 and ω (adiabatic constant) are constants and their values have been determined from dynamic experiments and are available in the literature for many common explosives. The values used for TNT are presented in Table 2.

Equation of State: JWL
Reference density $\rho = 1.658$ g/cm^3
$C_1 = 3.7377\ 10^8$ kPa
$C_2 = 3.73471\ 10^6$ kPa
$R_1 = 4.15$
$R_2 = 0.9$
$\omega = 0.35$
C-J detonation velocity: $6.93\ 10^3$ m/s
C-J energy/unit volumen: $6\ 10^6$ KJ/m^3
C-J pressure: $2.1\ 10^7$ kPa

Table 2: TNT properties

A shock equation of state combined with an elastoplastic strength model based on Drucker Prager criterion and a hydro tensile limit were used for the soil. The initial density was taken as $\rho = 2.2$ g/cm3 (wet density). The wet density was obtained considering a mean dry density of 2100 kg/m3 and a moisture content of 5%.

For non-cohesive soils, it could be necessary to use a shear modulus varying with depth. In absence of SPT data or other useful data such us Dynamic Cone Penetration Tests or Field Vane Test, a medium shear modulus in all depth was used.

A Drucker Prager criterion with standard values was adopted for the strength model. A summary of soil properties used for all the models is presented in Table 3

It is important to note that it was previously proved (Ambrosini et al. 2004) that the influence of the soil properties on the size of craters produced by explosive loads is usually rather small (variations of about ± 5% in crater diameter could be obtained).

Equation of State: Shock	Strength: Drucker Prager
Reference density $\rho = 2.2$ g/cm^3	
Gruneisen Gamma $\Gamma = 0.11$	
$c_o = 1.614\ 10^3$ m/s	
$S = 1.5$	
Shear Modulus $G = 2.4\ 10^5$ kPa	
Pressure 1 =-1.149 10^3 kPa	Yield stress 1 = 0 kPa
Pressure 2 = 6.88 10^3 kPa	Yield stress 2 = 6.2 10^3 kPa
Pressure 3 = 1.0 10^{10} kPa	Yield stress 3 = 6.2 10^3 kPa
Hydro tensile limit p_{min} = -100 kPa	

Table 3: Soil properties

In order to fulfill the radiation condition, a transmitting boundary was defined for air as well as soil subgrids external limits. The transmit boundary condition allows a stress wave to continue "through" the physical boundary of the subgrid without reflection. The size of the numerical mesh can be reduced by use of this boundary condition. The transmit boundary is only active for flow out of a grid.

2.4 Numerical results

The final state of the model is presented in Figure 5. The apparent diameter of the crater obtained is D=3.94m, practically coincident with experimental result.

The depth of the explosive load was varied from 25cm to 3m. The numerical models were modified in order to make them suitable for the different setups. The results obtained for the apparent crater diameter are consigned in Table 4. It should be noted that the crater diameter increases with increasing depth up to a certain depth. For deeper explosions the crater diameter decreases following Bull and Woodford (1999) observations. Figure 6 shows a typical camouflet obtained for 10 kg the TNT buried 3m that corresponds to $\lambda_c = 1.4$.

The results in Table 4 are also plotted in Figure 7 together with experimental results reported by Baker et al (1991) and Ambrosini et al (2002) and numerical results obtained for underground cylindrical charges (Luccioni and Ambrosini 2006). Although the types of soils involved and the shapes of the explosive loads are different, an excellent agreement between the present numerical results and those corresponding to Baker et al.(1991) and Ambrosini et al.(2002) can be observed in Figure 6.

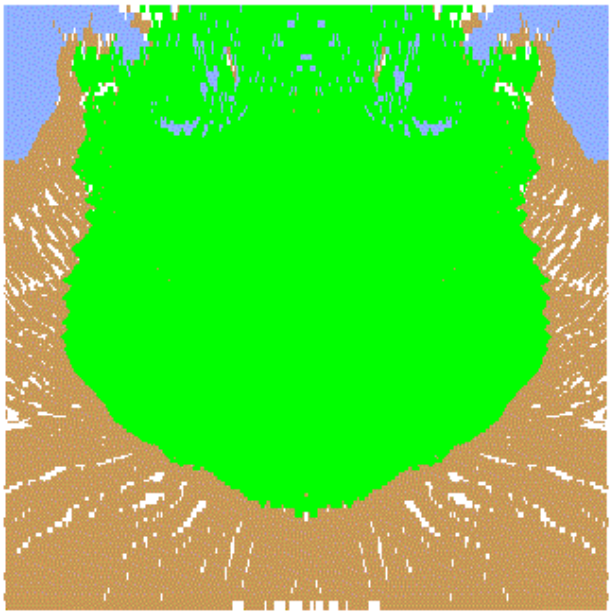

Figure 5 Crater obtained 10 kg of TNT buried 98 cm.

d [m]	$\lambda_c = \frac{d}{W^{1/3}}$ $\left[\mathrm{m}/kg^{1/3}\right]$	Apparent Crater diam D [m]
0.25	0.116	1.20
0.50	0.232	1.89
1.00	0.464	3.94
2.00	0.928	4.30
3.00	1.392	3.58

Table 4: Craters produced by 10 kg of TNT at different depths

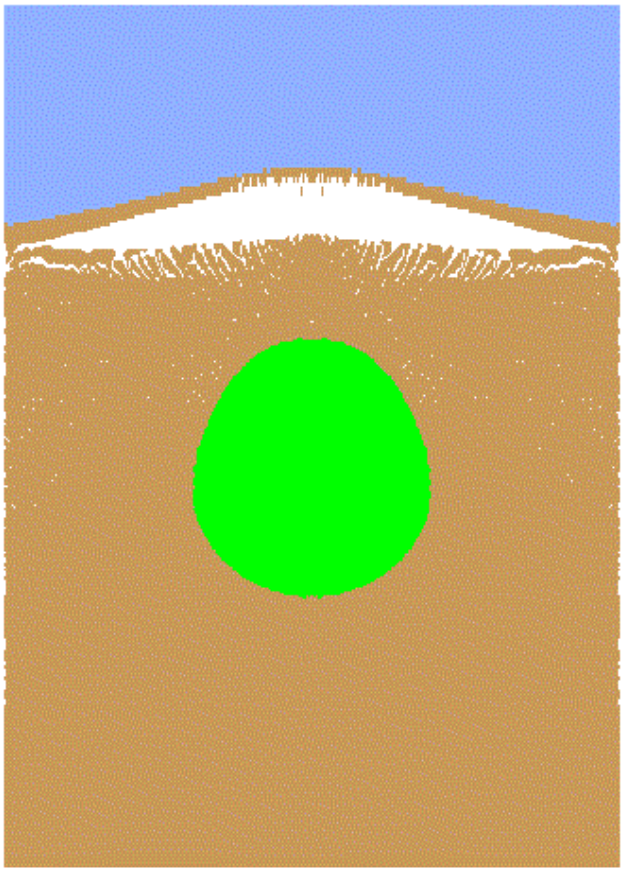

Figue 6. Cammouflet (10 kg of TNT at 3m depth)

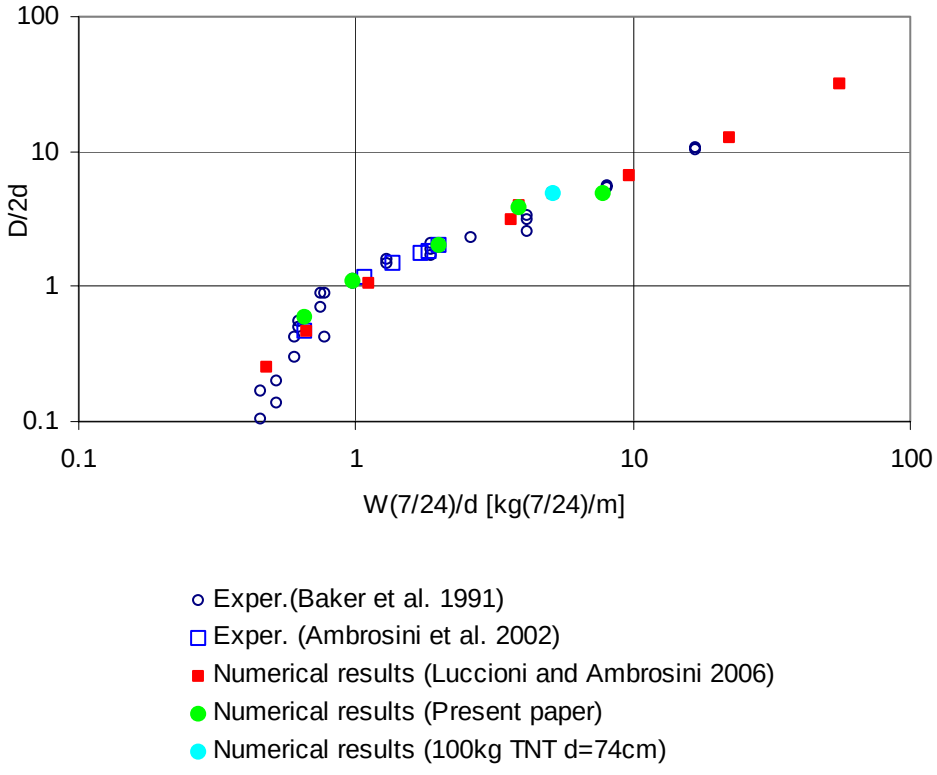

Figure 7. Variation of crater diameter with scaled distance. Comparison with experimental results.

3 EFFECT ON BURIED STRUCTURES

The propagation of the blast wave produced by underground explosions in soils and the effect on underground structures is analyzed in this section. For this purpose the numerical tests performed by Wang et al (2005) and Lu et al (2005) are numerically reproduced and the results are analyzed and compared.

3.1 100 kg of TNT at 74 cm depth (Wang et al 2005)

The detonation of an spherical TNT charge of 100 kg of TNT placed at 74 cm depth is analyzed in this section. The same computational program, processors and material models as those used in previous examples are first used. Figure 8 shows the model and the crater obtained for this blast event. The apparent crater diameter was D=7.24m. The point corresponding to this result was also plotted in Figure 7. A good agreement with experimental and previous numerical results is obtained.

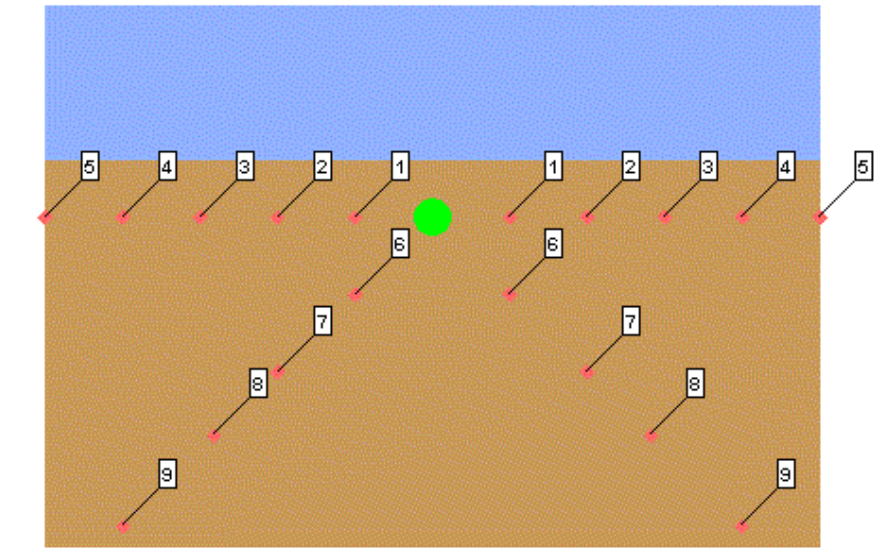

a)

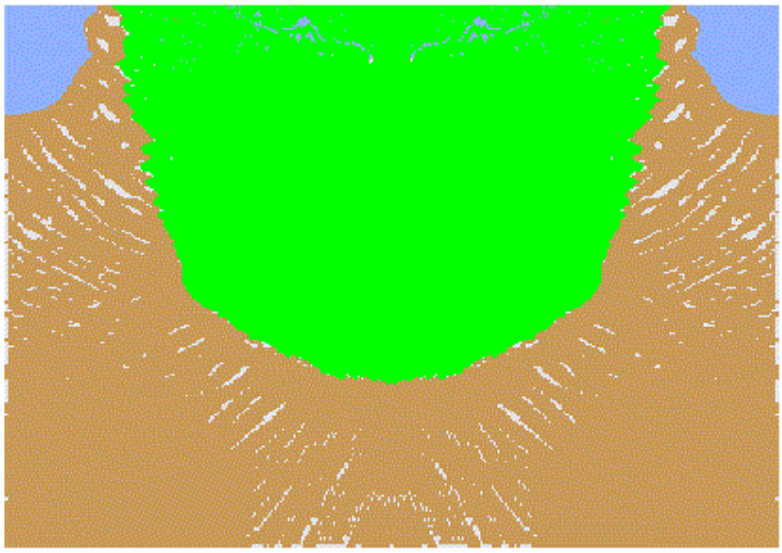

b)

Figure 8. 100 kg of TNT buried 74 cm a) Problem Setup b) Crater obtained.

The gauge points indicated in Figure 8 were defined in order to analyze the blast wave propagation in soil. All the variables of the problem were recorded in these points. A simple analysis of absolute velocity values at these points shows that these values y are very different from those presented by Wang et al (2005). The velocity values are strongly dependent on soil model and material properties. A new analysis was performed using a linear equation of state for the soil with the bulk modulus $K = 2.2\ 10^5$ kPa and $G = 1\ .5\ 10^5$ kPa. The apparent crater diameter obtained was the same. But this analysis leads to peak velocity values comparable with those presented by Wang et al (2005) for points 4 and 8 located at 4m from the charge. Nevertheless, the arrival time of the blast wave is different from that observed in that reference. The velocity history obtained for points 4 and 8 are represented in Figure 9.

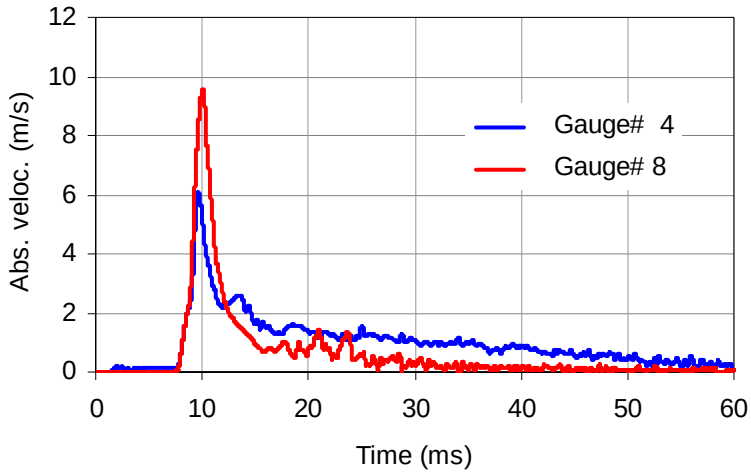

Figure 9. Absolute Velocity Histories

3.2 50 kg of TNT at 5m depth (Lu et al 2005)

The detonation of an spherical TNT charge of 50 kg of TNT placed at 5m depth is analyzed in this section. A linear equation of state was used for the soil with the bulk modulus $K = 2.2\ 10^5$ kPa and $G = 1\ .5\ 10^5$ kPa. Figure 10 shows the model and the camouflet obtained for this blast event. This case corresponds to $\lambda_c = 1.36$ and so a camouflet is expected to be formed. It can also be observed that the shape of the camouflet follows that suggested by Bull et al (1999) and presented in Figure 2. The camouflet comprises a spherical void and a conical shaped volume of subgrade had been displaced upwards, loosened and resettled. The surface disturbance due to a deep underground detonation is only a small elastic movement with very little mixing or disruption of the soil layers.

In order to measure the blast wave propagation in soil the gauge points indicated in Figure 10 are defined. The pressure and velocity values are recorded in these points. Figure 11 presents the pressure wave and the velocity wave at point 6 distant 10 m from the explosive charge. The peak values obtained for these variables and the arrival time of the blast wave are practically coincident with those obtained by Lu et al (2005). Once again a strong dependence on soil model and parameters is observed. Figure 12 shows the attenuation curves with scaled distance for pressure and velocity. The values suggested by TM5-855-1 (1984) are also plotted in this Figure. A good coincidence with these values is observed.

The problem is simulated again but with a rigid border in the lateral soil limit in order to

evaluate reflected pressures that are the pressures that would act on a structure placed in that location. Figure 11 also shows the pressure time histories for points 6 and 7. In this case the values obtained are 30% less than those reported by Lu et al (2005).

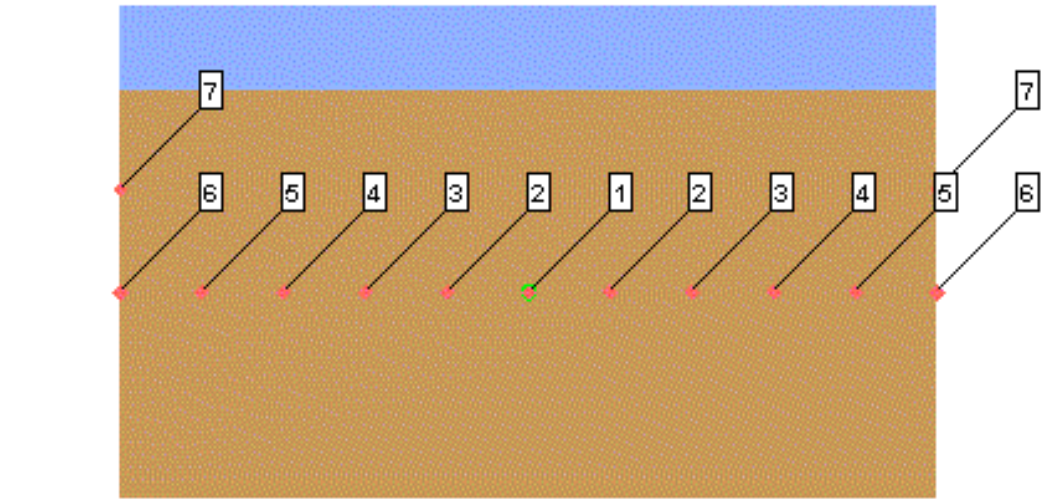

a)

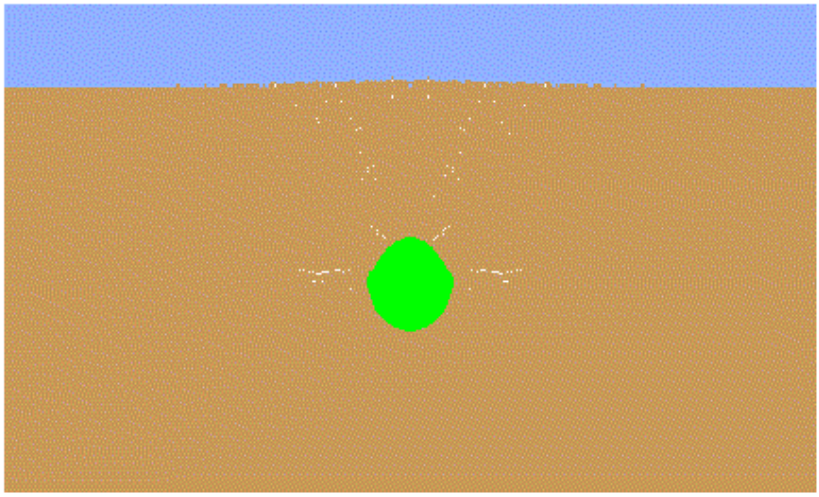

b)

Figure 10. 50 kg of TNT buried 4 m a) Problem Setup b) Camouflet (107 ms).

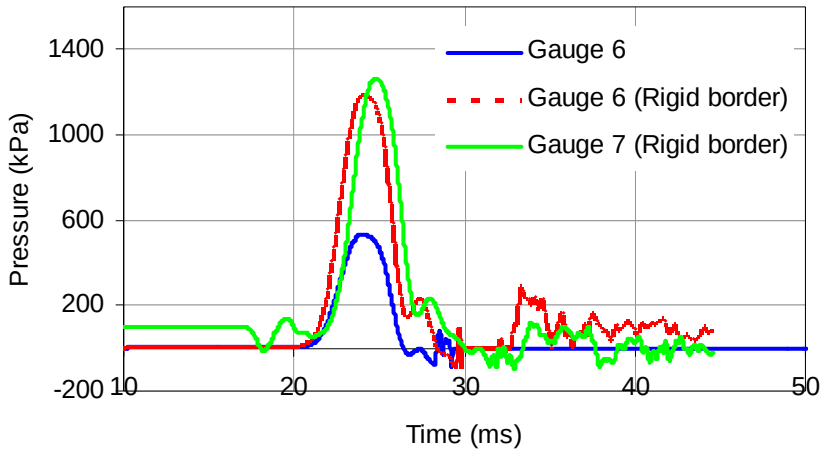

Figure 11. Pressures Histories

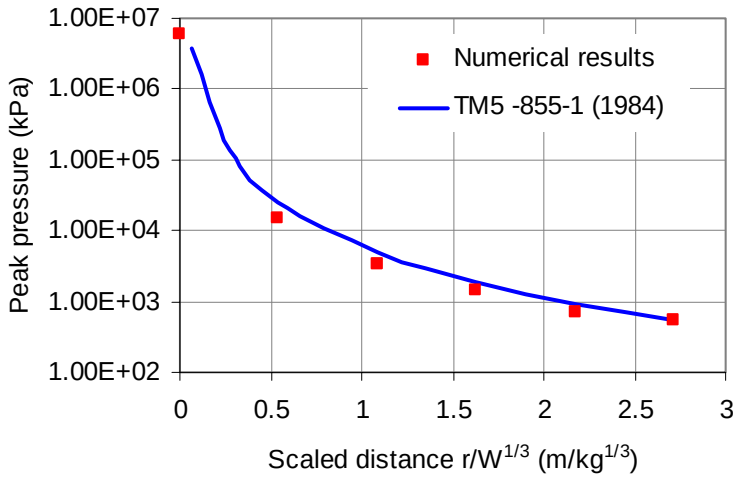

Figure 12. Blast Wave Attenuation with Distance From the Blast a) Peak Pressures b) Peak Velocity

4 EFFECT ON A STEEL PLATE OVER THE GROUND

4.1 Problem description

The tests performed by Hlady (2004) are numerically reproduced in this section. Tests were conducted with a simulated landmine in engineered soil containers where soil conditions could be carefully controlled. A target was attached to a piston apparatus, mounted above the soil container, and the energy transferred to the target was calculated from the height the piston jumped after the landmine was detonated. Variables included standoff, overburden, soil type, moisture, and density. High density, high moisture soil conditions produced seven times the energy transfer versus dry sand conditions.

The test setup is shown in Figure 13 (Hlady 2004). The target plate is 25.4 mm thick and 254 mm in diameter. The total mass of the target plate, mounting plate and shaft is 47 kg.

Steel soil containers filled with different soil with different moisture contents were used.

For all trials, the landmine was 25 g C4, encased in plastic, with a height-to diameter ratio of 35%. Different overburdens were tested from 0 to 150 mm were tested. Held (2002a) has done extensive research mapping the momentum distribution of AT landmines, in sand. Most of the damage results from momentum transfer from the sand to the target (Held 2002b) Therefore the ejecta is a significant source for the energy transfer to the target. When there is little or no overburden, the ejecta, and thus the energy transfer to the target, is reduced. Conversely, for large overburden, the soil is able to absorb a large amount of the explosive energy, and thus the amount of ejecta is reduced (in the extreme, an explosive buried deep underground does not produce any ejecta at all). Thus there exists an optimum overburden for energy transfer. The trend observed by Hlady (2004) indicates an optimum overburden, for 25 g of C4, in CFAS, to be about 50 mm.

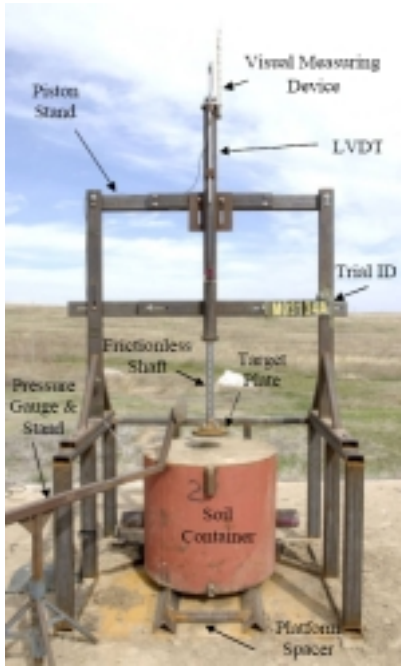

Figure 13. Test Setup (Hlady 2004)

4.2 Numerical Model

The numerical model used for this problem is presented in Figure 14. As the problem presents axial symmetry a 2D model is used. The soil, the air and the explosive are simulated with the same model and processors than in the other examples.

Taking into account that the TNT equivalence of c4 is 1.078 (TM5-855-1, 1984) , $W_{TNTequiv} = 1.078\ \ 25\text{g} = 26.95g$ TNT are used as explosive charge instead of a 25g of C4 used in the tests.

Only a 400 mm diameter and 270 mm height soil cylinder is modeled. This cylinder represents the central upper part of the soil container. Transmit boundaries conditions are assigned to the lateral and bottom sides of this cylinder in order to represents the rest of the soil surrounding this part. The target plate is model with a 254 mm diameter plate. The thickness of this plate is increased (118.4 mm) to represent the total mass of the target plate, the mounting plate and the shaft. Euler Lagrange interaction is defined to take into account

interaction of air, explosive and soil with the steel plate and the soil container.

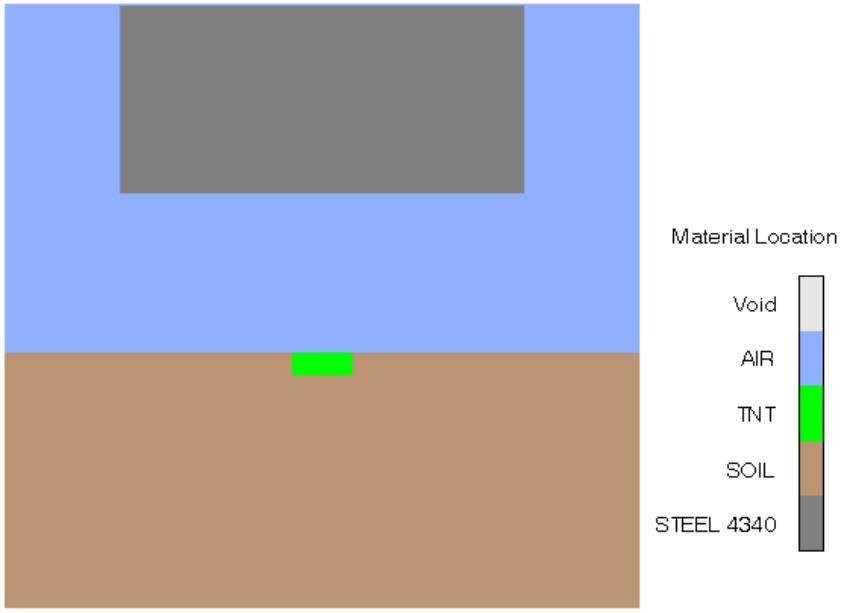

Figure 14. Numerical Model (0 overburden)

Two different types of soils were considered. Soil (a) and Soil (b) with the properties difined in Table 5. The two types of soil only differs in their elastic constants.

Equation of State: Linear	Strength: Drucker Prager	
Reference density $\rho = 2.2$ g/cm^3		
Bulk Modulus K	$K_a = 2.2\ 10^5$ kPa	$K_b = 3.52\ 10^5$ kPa
Shear Modulus G	$G_a = 1.5\ 10^5$ kPa	$G_b = 2.4\ 10^5$ kPa
Pressure 1 =-1.149 10^3 kPa	Yield stress 1 = 0 kPa	
Pressure 2 = 6.88 10^3 kPa	Yield stress 2 = 6.2 10^3 kPa	
Pressure 3 = 1.0 10^{10} kPa	Yield stress 3 = 6.2 10^3 kPa	
Hydro tensile limit p_{min} = -100 kPa		

Table 5: Soil Properties

The problem was run for different overburdens, from 0 to 150 mm. The variation of total energy transfer to the target plate for different overburdens is plotted in Figure 15 for soils 8a) and (b).

Figure 15. Energy Transfer to the Target Plate

5 CONCLUSIONS

A good agreement in crater diameter with experimental results obtained by other researchers and the authors has been obtained. The shape of the explosive load and the type of soil has practically non influence in the value of the crater diameter. Not only actual craters but also camouflets can be modeled.

Numerical results confirmed that the maximum crater diameter is obtained for $0.4<\lambda_c<0.6$.

Numerical results for the propagation of blast wave in soils are coincident with those suggested by codes and obtained by other authors. They are strongly dependent on the type of soil modeled. Consequently a more accurate model for soil should be defined in order to asses effect of buried explosions on underground structures or on structures placed over the ground.

6 AKNOWLEDGEMENTS

The financial support of the CONICET (Argentina) and CIUNT (National University of Tucumán) is gratefully acknowledged.

7 REFERENCES

Alia, A. and Souli, M., High explosive simulation using multi-material formulations. *Applied Thermal Engineering*, 26:1032–1042, 2006

Ambrosini, R.D., Luccioni, B. and Danesi, R., Riera, J. and Rocha, M.. Size of Craters Produced by Explosive Charges on or Above the Ground Surface. *Shock Waves*, 12(1):69-78, 2002.

Ambrosini, R.D., Luccioni, B. and Danesi, R.. Influence of the soil properties on craters produced by explosions on the soil surface. *Computational Mechanics*, XXIII:571-590, 2004.

Ambrosini, R.D. and Luccioni, B. Luccioni. Craters produced by explosions on the soil surface. *Journal of Applied Mechanics, ASME*, 73(6):890-900, 2006

AUTODYN, *Explicit Software for Non-Linear Dynamics*, Version 6.1, User's Manual. Century Dynamics Inc, 2005.

Baker W.E., Westine P.S. and Dodge FT. *Similarity methods in engineering dynamics*. Elsevier, Amsterdam, 1991

Bull, J.W. and Woodford, C.H. The effects of camouflets on subgrade surface support. Computer and Structures, 73:315-325, 1999.

Cheeseman, B.A., Wolf, S., Yen, C.F. and Skaggs, R. Blast simulation of explosives buried in saturated sand. *Fragblast*, 10 (1-2):1-8, 2006.

Formby, S.A. and Wharton, R.K. Blast characteristics and TNT equivalence values for some commercial explosives detonated at ground level. *Journal of Hazardous Materials,* 50:183-198, 1996.

Gupta, A.D. Estimation of vehicle floor plate loading and response due to detonation of a mine shallow-buried in dry sand and wet tuff Tuff. *US Army Ground Vehicle Survivability Symposium*, 1999.

Held, M. Momentum distribution of anti-tank mines, 20th International Symposium on

Ballistics, Orlando, 2002a.
Held, M. Calibration tests for blast impulse loads on anti-tank mines. MABS17, Las Vegas, 2002b.
Hlady, S. L. Effect of soil parameters on land mine blast. *18th Military Aspects of Blast and Shock (MABS) Conference*, Germany.2004.
Lee, E.L. and Tarver, C.M.. Phenomenological model of shock initiation in heterogeneous explosives. *Physics of Fluids*, 23(12):2362-2372, 1980.
Lu, Y., Wang, Z. and Chong, K. A comparative study of buried structure in soil subjected to blast load using 2D and 3D numerical simulations. *Soil Dynamics and Earthquake Engineering,* 25:275–288, 2005.
Luccioni, B. and Ambrosini, R.D. Craters produced by underground explosions. Computational Mechanics, XXV:1603-1614, 2006.
TM5-855-1. Fundamental of protective design for conventional weapons. *US Army Engineer Waterways Experiment Station*, Vicksburg; 1984.
Wang, Z., Lu, Y., Hao, h. and Chong, K. A full coupled numerical analysis approach for buried structures subjected to subsurface blast. *Computers and Structures,* 83:339–356, 2005.